Hindawi Publishing Corporation
Journal of Nanomaterials
Volume 2013, Article ID 372951, 5 pages
http://dx.doi.org/10.1155/2013/372951

Research Article

Synthesis, Characterization, and Photocatalysis of ZnO and Er-Doped ZnO

Kai-sheng Yu,[1,2] Jian-ying Shi,[3] Zai-li Zhang,[1,2] Yong-mei Liang,[1,2] and Wei Liu[1,2]

[1] *School of Environmental Science and Engineering, Sun Yat-sen University, Guangzhou 510275, China*
[2] *Guangdong Province Key Laboratory of Environmental Pollution Control and Remediation Technology, Guangzhou 510275, China*
[3] *School of Chemistry and Chemical Engineering, Sun Yat-sen University, Guangzhou 510275, China*

Correspondence should be addressed to Wei Liu; esslw@mail.sysu.edu.cn

Received 30 March 2013; Accepted 8 July 2013

Academic Editor: Xuedong Bai

ZnO and Er-doped ZnO with different molar ratios of Er/Zn were prepared using the homogeneous precipitation method. The photocatalysts prepared were characterized using scanning electron microscopy, transmission electron microscopy, X-ray diffraction (XRD), UV-vis spectroscopy, and photoluminescence spectroscopy. The results showed that the Er-doped ZnO displayed characteristic wurtzite-type peaks in the XRD spectra. The Er-doped ZnO absorbed much more light than ZnO in the ultraviolet region. And the doping of Er into ZnO enhanced the intensity of the fluorescence emission. The degradation of methylene blue (MB) solution demonstrated that the photocatalytic activity of ZnO was significantly improved with Er doping.

1. Introduction

ZnO is a semiconductor with a wide band gap (3.3 eV) and a large exciton binding energy and is abundant in nature and environmentally friendly; these characteristics make this material attractive for many applications, including solar cells, optical coatings, photocatalysts, and electrical devices [1]. Researches have shown that ZnO exhibits better photocatalytic efficiency than TiO_2 for the removal of organic compounds in water matrices [2]. ZnO-based photocatalysts have received much attention because of their excellent properties, which include their high chemical stability, their nontoxicity, and their abundance in nature.

Recently, environmental problems such as air and water pollution have provided the impetus for sustained fundamental and applied research in the area of environmental remediation. ZnO has proven attractive as a photocatalyst material, because it shows high catalytic efficiency and is of low-cost and environmentally sustainable [3, 4]. ZnO has emerged as a more efficient catalyst for the detoxification of water, because it generates H_2O_2 more efficiently [5], and it has high reaction and mineralization rates. It also has a higher number of active sites with high surface reactivity. ZnO has been demonstrated as an improved photocatalyst compared with commercialized TiO_2, based on its larger initial activity rates, and its efficient absorption of solar radiation. However, ZnO has almost the same band gap (3.2 eV) as TiO_2. The modification of ZnO via doping with metal ions has been developed as an effective method to promote photocatalytic activity [6–9]. There have been many studies reporting the optical properties of Er-doped ZnO, and some of them specifically, the photocatalysis of Er-doped ZnO [9–15].

This paper reports a simple route for the preparation of undoped and Er-doped zinc oxide nanoparticles via the chemical precipitation method. The prepared nanoparticles were characterized and then used as a photocatalyst in the photodegradation of methylene blue. Methylene blue is a blue, organic cationic thiazine dye that has been commonly employed as a model dye to evaluate the photocatalytic activity among other photosensitizing dyes like eosin Y, pyrene, and so forth.

2. Experimental

2.1. Synthesis. Homogeneous precipitation [10] is one of the most successful and easy to conduct techniques for

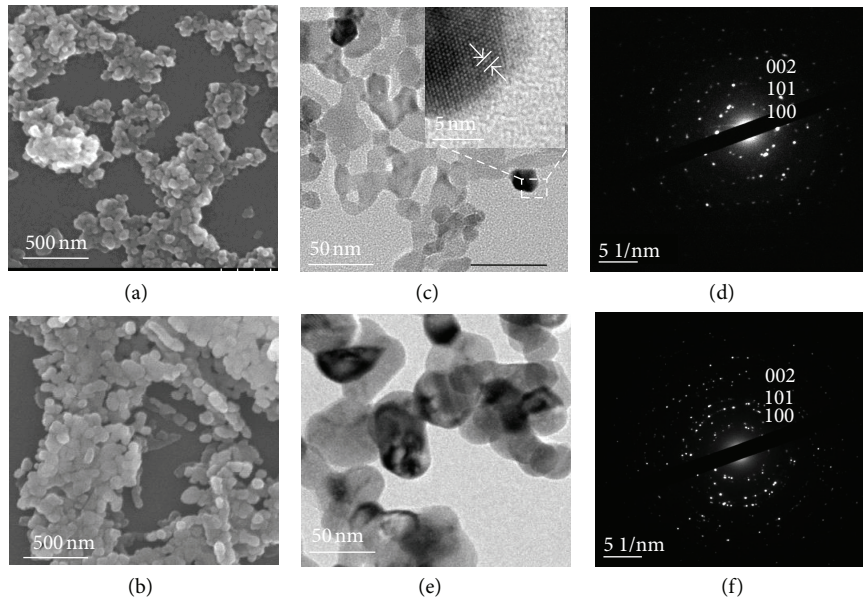

Figure 1: (a), (c), (d) SEM/TEM image of ZnO. (b), (e), (f) SEM/TEM image of Er-doped ZnO.

synthesizing Er-dopped ZnO powders among solid-state reaction method [9, 15], the spray deposition technique method [11], sol-gel method [13], and so forth. Briefly, with urea as a precipitating agent, erbium nitrate (AR, 99.99%) and zinc acetate were added to a water bath at 80°C and heated for 4 h. This mixture was then left to cool and settle for half an hour; this was followed by centrifugal separation and successive washing with deionized water and anhydrous alcohol, which was repeated five times. Drying was performed at 80°C for 2 h, in a vacuum drying oven, producing the nanometer-sized ZnO precursor. Finally, this precursor was calcined in a muffle at 600°C for 4 h, which produced the nanometer-sized ZnO powder.

2.2. Characterization. The phase identity and crystalline size of the ZnO nanoparticles were determined using an X-ray diffractometer (XRD). A scanning electron microscope (SEM) was used to make morphological observations on the ZnO and Er-doped ZnO nanoparticles. The optical properties of the samples were investigated by measuring the UV-vis absorbance spectra and photoluminescence spectrum at room temperature. The photocatalytic activity of the ZnO powders was evaluated by measuring the degradation of methylene blue (MB) in water, in the UV region.

2.3. Photocatalytic Activity. The photocatalytic activity of the ZnO and Er-doped ZnO was determined by measuring the degradation of MB solution under UV illumination (32 W). The reaction was carried out with 0.05 g of photocatalyst suspended in a 100 mL MB solution. The initial concentration of the MB solution was 10 mg/L. Before the UV lamps were turned on to start the illumination, the solution was stirred for 0.5 h in the dark, to establish an adsorption/desorption equilibrium between the photocatalysts and the dye. The solution was sampled at 20 min intervals and centrifuged to remove any sediment, and then monitored using UV-vis spectroscopy.

3. Results and Discussion

3.1. Scanning Electron Microscopy (SEM)/Transmission Electron Microscopy (TEM). The SEM images in Figures 1(a) and 1(b) show the size and distribution of the ZnO and Er-doped ZnO particles; the grain was smooth, the product showed no sintering reunion phenomena, and there was a narrow particle size distribution. The SEM investigations revealed that the crystallites were of nanometer size in all of the samples, but no significant change was observed in the particle size for the Er-doped particles. The average diameter was calculated as ~45 nm; the nanometer size of the particles led to an increased surface area and a consequent increase in the number of photocatalytic reaction sites, properties that improved the photocatalytic activity. Figures 1(c) and 1(e) compare the TEM images for the ZnO and the Er-doped ZnO. The sizes were similar, which agreed well with the results from the diameter measurements. The selected area electron diffraction (SAED) patterns shown in Figures 1(d) and 1(f) for the ZnO and Er-doped ZnO revealed the polycrystalline nature of the materials, which could be well-indexed to diffractions from the (100), (002), and (101) planes of the hexagonal wurtzite structure. Furthermore, the difference in scattered spots between Figures 1(d) and 1(f) clearly showed the presence of secondary phase in addition to the wurtzite ZnO.

3.2. X-Ray Diffraction Patterns (XRD). The XRD patterns for the Er-doped ZnO are shown in Figure 2, for different doping concentrations of Er. The sharp and intense peaks indicated that the samples were highly crystalline, and that the ZnO nanoparticles had a polycrystalline structure. The peaks were

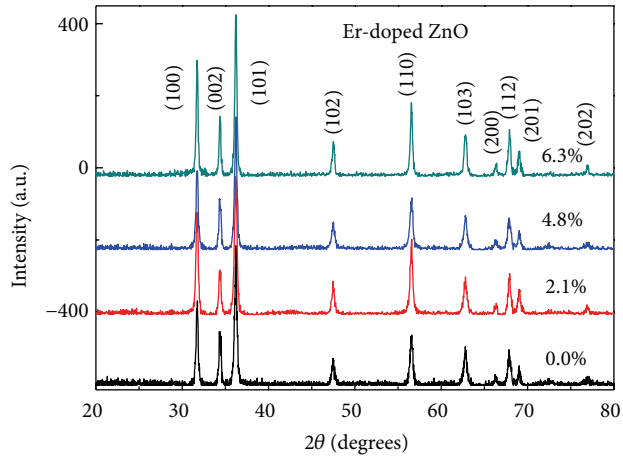

Figure 2: XRD patterns for ZnO and Er-doped ZnO with different doping concentrations.

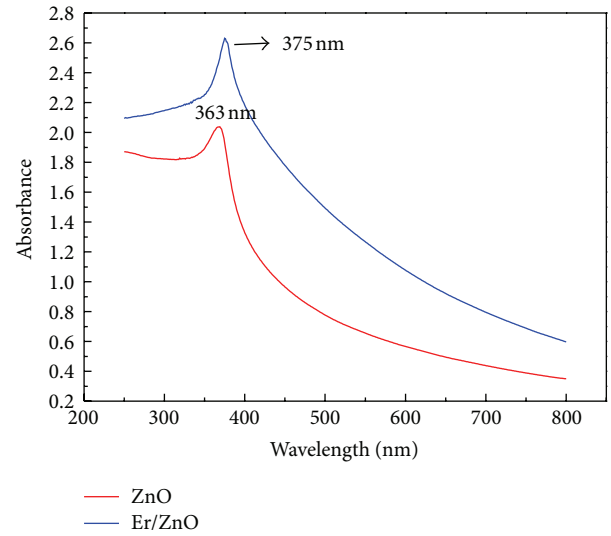

Figure 3: UV-vis spectra for ZnO and the Er-doped ZnO nanocomposites.

at 31.8°, 34.4°, 36.3°, 47.5°, 56.6°, 62.9°, 66.4°, 68.0°, 69.1°, and 77.0° and were indexed to the (100), (002), (101), (102), (110), (103), (200), (112), (201), and (202) planes of the ZnO crystal given by the standard data file (JCPDS file no. 36-1451). The XRD peaks for the (100), (002), and (101) planes indicated the formation of a pure-phase wurtzite ZnO structure. The XRD analysis further showed that the main diffraction peaks for the Er-doped ZnO composites were similar to those for the pure ZnO and corresponded to the hexagonal phase of ZnO; this was in good agreement with the SAED results. According to the recent report [15], the shifted peaks in XRD studies revealed the occurrence of secondary phase in Er-dopped ZnO by solid-state reaction method with Er^{3+} content >1%. In this case, the peaks corresponding to the secondary phase in Figure 2 were not obvious. This is probably because of the doped Er^{3+} ions mainly substituted regular Zn^{2+} lattice sites (the ionic radius of Er^{3+} is smaller than the ionic radius of Zn^{2+}) by homogeneous precipitation method.

3.3. Ultraviolet and Visible Absorption Spectra (UV-vis). UV-vis spectra were measured for ZnO and Er/ZnO in the wavelength region of 200–800 nm, and the results are shown in Figure 3. The pure ZnO showed a maximum absorption peak at 363 nm, and the absorption was mainly concentrated in the ultraviolet region, with less visible light absorption. The absorption band near 363 nm was due to the transition of electrons from the valence band to the conduction band. UV-vis spectra of Er/ZnO composite material showed a slightly redshifted peak at 375 nm. This indicated an ineffective impurity band that was introduced by Er dopping [16].

It can be speculated that the metal ions were in the internal ZnO lattice and that the interaction of the doping ions with the ZnO destroyed part of the original lattice, forming lattice defects and making the ZnO absorption edge mobile, similar to results reported in the literature [17]. The redshift in the absorption wavelength range and the increase in the absorption intensity showed that the rate of formation of electron-hole pairs on the catalyst surface increased greatly, resulting in the catalyst exhibiting a higher photocatalytic efficiency. The reason for the redshift in the absorption wavelength range for the Er-doped ZnO was likely the formation of defect energy levels between the valence and conduction bands in the ZnO band structure. This would have played an important role in improving the catalytic activity of the ZnO.

3.4. Photoluminescence Spectra. Photocatalysts generate electrons and holes after being activated by light, and the recombination of some electrons and holes can release energy in the form of fluorescence emission.

Figure 4 shows room-temperature PL spectra for ZnO and the Er-ZnO nanocomposites containing different Er contents. All of the spectra showed two emission bands located at 396 and 484 nm. While the sharper 396-nm emission band has typically been assigned to the near-band-edge emission in ZnO [18], the band in the visible spectral range (showing a peak at 484 nm) has been attributed to the recombination of photogenerated holes with singly ionized charge states of the intrinsic defects such as oxygen vacancies, Zn interstitials, or impurities [19–22].

The characteristics of the PL spectra for the Er-doped ZnO nanocomposites were very similar to those of the spectra for the ZnO without Er. However, the intensity of the excitonic emission band increased compared with that for the ZnO without Er. This can be explained by the formation mechanism and structure of the Er-doped ZnO nanoparticles. Er^{3+} would have been removed from the conduction band of ZnO by the accumulated electrons and deposited on ZnO surface, and Er^{3+} requires three electrons for the reduction of each ion, and this would have resulted in more and more ZnO particles becoming attached together. This accumulation of ZnO particles in the presence of Er^{3+} would have caused an increased local concentration of excitons during photoexcitation, thus resulting in an increased excitonic emission intensity compared with the

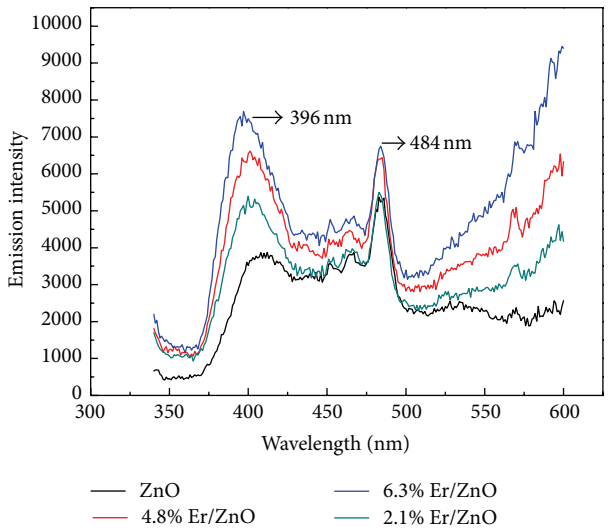

Figure 4: PL spectra of the Er-doped ZnO nanocomposites with different Er concentrations.

undoped ZnO. The fluorescent light intensity was therefore enhanced with increasing Er contents.

The heavily doped product showed an extremely high PL intensity in the present case, which might have been related to the interaction between ZnO and Er. The majority of Er in the ZnO was likely associated with rare earth elements occupying substitutional Zn sites [23]. However, we did not observe Er^{3+} emission peaks. It is possible that weak Er^{3+} ion emission peaks were embedded in the signal from a strong, deep-level emission. The doping of metals and/or transition metals increases the number of surface defects and the surface area and surface defects play an important role in the photocatalytic activity of metal oxides.

3.5. Photocatalytic Activity. As Figure 5 shows, when the pure-phase, nanometer-sized ZnO was placed in a photocatalytic MB solution for 1 h, the degradation rate was 69.28%; with Er doping contents of 2.1%, 4.8%, and 6.3%, the photocatalysis degradation rates were 86.3%, 97.7%, and 91.3%, respectively. However, the photocatalytic degradation rate of the composite photocatalyst with a doping concentration of 6.3% was lower than that of the photocatalyst with a doping concentration of 4.8%.

Similar to metal doping, the use of rare earth ions provides electron traps that suppress electron-hole recombination. The holes are then able to migrate towards the surface of the catalyst and oxidize the adsorbed organic compounds [24, 25]. The Er-doping of the nanometer-sized ZnO catalyst resulted in increased fluorescence emission, and increases in the electron-hole pair concentration. The Er ions provided a favorable redox potential, which resulted in the photoproduction of electronic defects and the inhibition of electron-hole recombination. The surface favored the generation of positive holes, which were considered to be the active center of the reaction; hence, the excellent generation of holes led in turn to the effective removal of the MB dye.

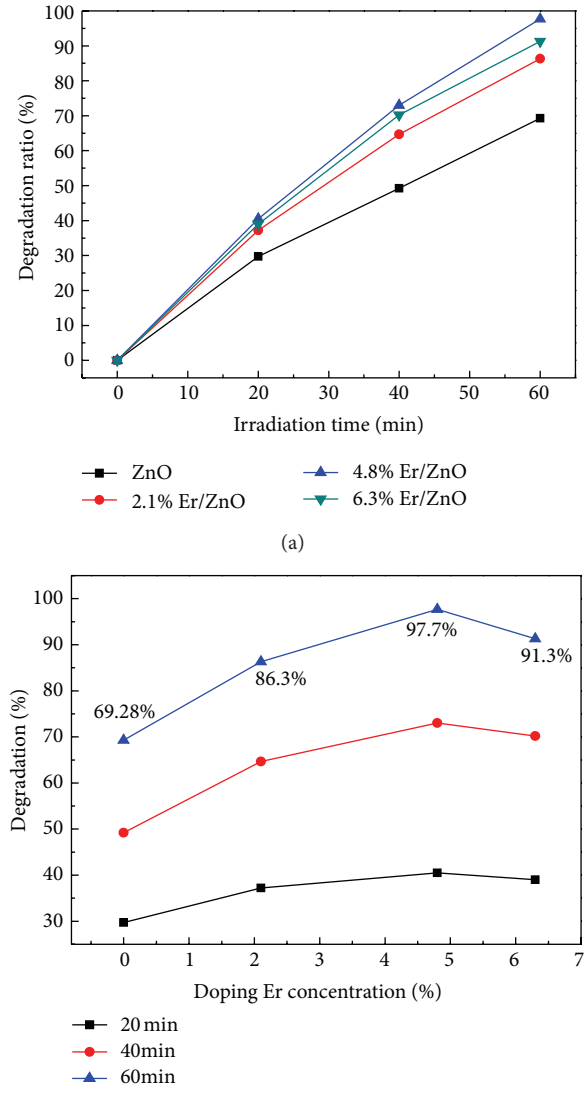

Figure 5: (a) Photocatalytic degradation curve for ZnO and Er-doped ZnO under UV-light irradiation; (b) degradation rates of Er-doped ZnO with different Er concentrations.

However, the photocatalytic experiments showed that the photocatalytic effects did not increase monotonically as the doping amount was increased; the effects began to decrease when the Er content was increased to 6.3%. This phenomenon was mainly due to the fact that when the rare earth ion concentration was increased to a certain level, the light penetrated into the ZnO past the space-charge layer, and the effective separation of the light-generated electron-hole pairs was suppressed. Accordingly, there is an optimal concentration of dopant ions; at this concentration, the thickness of the space-charge layer and the depth of the light penetration were similar. Further, too high a quantity of rare earth ions on the surface of the ZnO also increased the recombination of electron-hole pairs, thereby reducing the photocatalytic activity.

4. Conclusion

ZnO and Er-doped ZnO photocatalysts with different molar ratios of Er/Zn were prepared via the homogeneous precipitation method and consisted of wurtzite-type ZnO. The doping of Er into the ZnO expanded the range of absorption and enhanced the intensity of the fluorescence emission with increasing the surface area and surface defects, which played an important role in promoting the photocatalytic activity of the ZnO. The results of the experiments showed that doping Er into ZnO modified the optical properties of the ZnO and greatly improved the photocatalytic activity of the ZnO. This study of Er modified ZnO provides theoretical and methodological support for improving the photocatalytic activity of photocatalyst in the future.

References

[1] M. Nirmala and A. Anukaliani, "Synthesis and characterization of undoped and TM (Co, Mn) doped ZnO nanoparticles," *Materials Letters*, vol. 65, no. 17-18, pp. 2645–2648, 2011.

[2] S. Anandan, A. Vinu, K. L. P. Sheeja Lovely et al., "Photocatalytic activity of La-doped ZnO for the degradation of monocrotophos in aqueous suspension," *Journal of Molecular Catalysis A*, vol. 266, no. 1-2, pp. 149–157, 2007.

[3] P. V. Kamat, "Photochemistry on nonreactive and reactive (semiconductor) surfaces," *Chemical Reviews*, vol. 93, no. 1, pp. 267–300, 1993.

[4] E. Pelizzetti and N. Serpone, *Homogeneous and Heterogeneous Photo-Catalysis*, Reidel, Dordrecht, The Netherlands, 1986.

[5] E. R. Carraway, A. J. Huffman, and M. R. Hoffmann, "Photocatalytic oxidation of organic acids on quantum-sized semiconductor colloids," *Environmental Science and Technology*, vol. 28, no. 5, pp. 786–793, 2004.

[6] M. G. Nair, M. Nirmala, K. Rekha, and A. Anukaliani, "Structural, optical, photo catalytic and antibacterial activity of ZnO and Co doped ZnO nanoparticles," *Materials Letters*, vol. 65, no. 12, pp. 1797–1800, 2011.

[7] H. Li, Z. Zhang, J. Huang, R. Liu, and Q. Wang, "Optical and structural analysis of rare earth and Li co-doped ZnO nanoparticles," *Journal of Alloys and Compounds*, vol. 550, pp. 526–530, 2013.

[8] Y. Liu, W. Luo, R. Li, G. Liu, M. R. Antonio, and X. Chen, "Optical spectroscopy of Eu^{3+} doped ZnO nanocrystals," *Journal of Physical Chemistry C*, vol. 112, no. 3, pp. 686–694, 2008.

[9] J. C. Ronfard-Haret, "Electric and luminescent properties of ZnO-based ceramics containing small amounts of Er and Mn oxide," *Journal of Luminescence*, vol. 104, no. 1-2, pp. 1–12, 2003.

[10] A. K. Pradhan, K. Zhang, G. B. Loutts, U. N. Roy, Y. Cui, and A. Burger, "Structural and spectroscopic characteristics of ZnO and ZnO:Er^{3+} nanostructures," *Journal of Physics Condensed Matter*, vol. 16, no. 39, pp. 7123–7130, 2004.

[11] J. Ebothe, W. Gruhn, A. Elhichou, I. V. Kityk, R. Dounia, and M. Addou, "Giant piezooptics effect in the ZnO-Er^{3+} crystalline films deposited on the glasses," *Optics and Laser Technology*, vol. 36, no. 3, pp. 173–180, 2004.

[12] W. C. Yang, C. W. Wang, J. C. Wang et al., "Aligned Er-doped ZnO nanorod arrays with enhanced 1.54 μm infrared emission," *Journal of Nanoscience and Nanotechnology*, vol. 8, no. 7, pp. 3363–3368, 2008.

[13] V. Kumari, V. Kumar, B. P. Malik, R. M. Mehra, and D. Mohan, "Nonlinear optical properties of erbium doped zinc oxide (EZO) thin films," *Optics Communications*, vol. 285, no. 8, pp. 2182–2188, 2012.

[14] J. C. Sin, S. M. Lam, K. T. Lee, and A. R. Mohamed, "Fabrication of erbium-doped spherical-like ZnO hierarchical nanostructures with enhanced visible light-driven photocatalytic activity," *Materials Letters*, vol. 91, pp. 1–4, 2013.

[15] J. Rita and R. Rajaram, "Synthesis and characterization of rare earth ion doped Nano ZnO," *Nano-Micro Letters*, vol. 4, no. 2, pp. 65–72, 2012.

[16] C. F. Zhe, *Handbook of Zinc Oxide and Related Materials*, CRC Press, Taylor & Francis, Boca Raton, Fla, USA, 2013.

[17] Y. Ling, W. Jiang, X. Wu, and X. Bai, "Preparation and visible light photocatalytic properties of (Er, La, N)-Codoped TiO_2 nanotube array films," *Journal of Nanoscience and Nanotechnology*, vol. 9, no. 2, pp. 714–717, 2009.

[18] S. Y. Bae, C. W. Na, J. H. Kang, and J. Park, "Comparative structure and optical properties of Ga-, In-, and Sn-doped ZnO nanowires synthesized via thermal evaporation," *Journal of Physical Chemistry B*, vol. 109, no. 7, pp. 2526–2531, 2005.

[19] U. Ozgour, Y. I. Alivov, C. Liu et al., "A comprehensive review of ZnO materials and devices," *Journal of Applied Physics*, vol. 98, no. 4, Article ID 041301, 103 pages, 2005.

[20] D. C. Look, "Recent advance in ZnO materials and devices," *Materials Science and Engineering B*, vol. 80, pp. 383–387, 2001.

[21] T. Parvin, N. Keerthiraj, I. A. Ibrahim, S. Phanichphant, and K. Byrappa, "Photocatalytic degradation of municipal wastewater and brilliant blue dye using hydrothermally synthesized surface-modified silver-doped ZnO designer particles," *International Journal of Photoenergy*, vol. 2012, Article ID 670610, 8 pages, 2012.

[22] D. Zhang and F. Zeng, "Visible light-activated cadmium-doped ZnO nanostructured photocatalyst for the treatment of methylene blue dye," *Journal of Materials Science*, vol. 47, no. 5, pp. 2155–2161, 2012.

[23] U. Wahl, E. Rita, J. G. Correia, E. Alves, and J. P. Araújo, "Implantation site of rare earths in single-crystalline ZnO," *Applied Physics Letters*, vol. 82, no. 8, pp. 1173–1175, 2003.

[24] P. K. Dutta, S. O. Pehkonen, V. K. Sharma, and A. K. Ray, "Photocatalytic oxidation of arsenic (III): evidence of hydroxyl radicals," *Environmental Science and Technology*, vol. 39, no. 6, pp. 1827–1834, 2005.

[25] L. Zhang and Y. Zhu, "A review of controllable synthesis and enhancement of performances of bismuth tungstate visible-light-driven photocatalysts," *Catalysis Science and Technology*, vol. 2, no. 4, pp. 694–706, 2012.